Determination of the Newtonian gravitational constant *G* with a nonlinear fitting method

Jun Luo,* Zhong-Kun Hu, Xiang-Hui Fu, and Shu-Hua Fan
Center for Gravitational Experiment, Huazhong University of Science and Technology, Wuhan 430074, People's Republic of China

Meng-Xi Tang
Department of Physics, Zhongshan University, Guangzhou 510275, People's Republic of China
(Received 17 April 1998; published 30 December 1998)

The Newtonian gravitational constant G is determined by means of a high-Q torsion pendulum and the time-of-swing method, in which the period of the pendulum is altered by the presence of two 6.25-kg stainless steel cylinders. The nonlinear fitting method is used to extract the frequencies from the angle-time data of the pendulum. The resulting value of G is $(6.6699\pm0.0007)\times10^{-11}$ m^3 kg^{-1} s^{-2}. [S0556-2821(98)06924-0]

PACS number(s): 04.80.Cc, 02.60.Ed, 06.20.Jr

I. INTRODUCTION

Improvements in our knowledge of the absolute value of the Newtonian gravitational constant G have come very slowly over the years [1], and G is still the least precisely determined fundamental constant and some recent results have a fractional discrepancy as large as 6×10^{-3} [2–5]. In the experiments measuring G, the torsion pendulum is a mainstay instrument, and the time-of-swing method has commonly been used [6,7] although some other methods have also been employed and proposed [3,8,9]. This is because the time-of-swing method, as compared with the direct deflection method, is not so sensitive to the drift of the equilibrium position of the pendulum and the quantities to be measured are all stationary values. Because of the advantages stated above, we have also determined the Newtonian gravitational constant G by the time-of-swing method with a high-Q torsion pendulum recently. For a study of nonlinear effect, the torsion pendulum system was designed to be sensitive to the inhomogenous gravitational fields produced by both the surrounding bodies and the attracting masses in our experiment, and then the nonlinear fitting method was employed to extract the frequencies from the angle-time data of the pendulum.

The time-of-swing method is based on detecting the change in torsional oscillation frequency at different configurations of attracting masses. In their absence, the square of free oscillation frequencies ω_0 is related to the moment I and fiber torsion constant K_f by

$$\omega_0^2=K_f/I. \tag{1}$$

The ''gravitational torsion constant'' contributed by the interaction gravitational potential energy of the pendulum and attracting masses, $V_g(\varphi)$, can be expressed as

$$K_g(\varphi)=\frac{\partial^2 V_g(\varphi)}{\partial\varphi^2}\equiv C_g(\varphi)G, \tag{2}$$

where φ is the angle between the axes of the pendulum beam and the attracting masses, and $C_g(\varphi)$ is calculated from the geometry, positions, and densities of the pendulum and attracting masses. Therefore, the frequency of small oscillation of the pendulum is

$$\omega_{g0}^2(\varphi)=[K_f+K_g(\varphi)]/I. \tag{3}$$

Most time-of-swing method experiments are selected with the near position configuration when the pendulum is in line with the source masses ($\varphi=0$) and far position ($\varphi=\pi/2$) configuration [13]. Because the gravitational force cannot be screened, the inhomogenous background gravitational field produced by the surrounding masses also contributes a gravitational torsion constant $K_b(\varphi)$: therefore, Eqs. (1) and (3) should be rewritten as

$$\omega_0^2(\varphi)=[K_f+K_b(\varphi)]/I, \tag{4}$$

$$\omega_{g0}^2(\varphi)=[K_f+K_b(\varphi)+K_g(\varphi)]/I, \tag{5}$$

where $K_b(\varphi)$ cannot be precisely calculated and it is also very difficult to keep it as a constant both at near position and far position configurations. For example, any asymmetry and inhomogeneity of the rotary table will lead to a systematic error if the experiment was designed to measure the frequency difference between the attracting masses at near and far positions. In our experiment, $\Delta(\omega_0^2)=\omega_{g0}^2-\omega_0^2$ is determined by measuring the frequencies of the torsion pendulum with and without the attracting masses in position, and the systematic error due to the asymmetry and inhomogeneity of the table can be avoided because the table is at rest during the experiment. The gravitational constant G is therefore given by

$$G=(\omega_{g0}^2-\omega_0^2)I/C_g. \tag{6}$$

The time-of-swing method has many advantages and was widely used in the determination of the Newtonian gravitational constant, but it has some shortcomings at the same time. First, in this method there are the important nonlinear effects in the motion of the pendulum itself, independent of any defect in a detector, caused by the finite amplitude of the swing and the inhomogeneities of both the gravitational field

*Email address: jluo@blue.hust.edu.cn

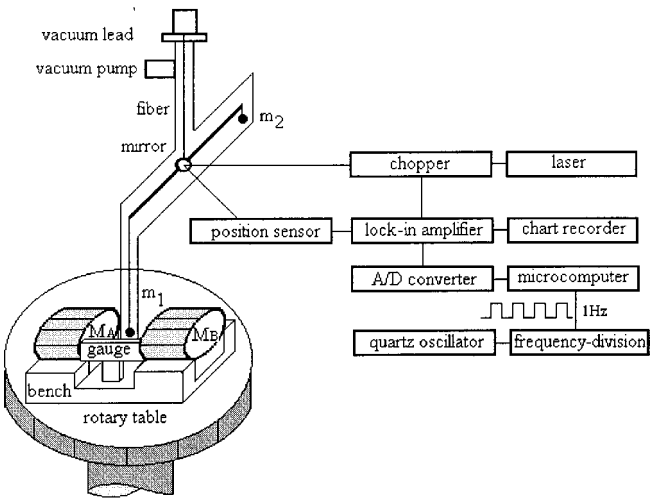

FIG. 1. Schematic of the apparatus used in the determination of G.

of the attracting masses and the background gravitational field. The nonlinear effect can be reduced at small amplitudes, but the smaller the amplitude, the lower the precision of measurement of the period. The nonlinear effect due to the attracting masses can also be reduced through an optimum positioning of the pendulum and attracting masses [10,11], but it is difficult to reduce the nonlinear effect due to the local inhomogeneity of the background gravitational field. So the pendulum will mainly oscillate at the fundamental frequency and also with high-order harmonic frequencies. This means that a nonlinear fitting method should be used in data processing. Second, Kuroda [12] pointed out that the time-of-swing method may have a systematic bias due to torsion fiber anelasticity, and this upward fractional bias should be $1/\pi Q$. Bagley and Luther [13] tested this hypothesis recently. Therefore, a high-Q torsion pendulum is used in our experiment to decrease this systematic bias.

II. TORSION PENDULUM SYSTEM

A schematic diagram of the apparatus is shown in Fig. 1, and the corresponding dimensions and masses are listed in Table I. The two separated cylindrical attracting masses, marked M_A and M_B, are fabricated from nonmagnetic stainless steel and have been used by Chen *et al.* in the Cavendish laboratory of Cambridge [14]. They are located on opposite sides of the copper spherical test mass m_1, which hangs from one end of the aluminum beam by a 25-μm tungsten wire about 435 mm long. The counterweight m_2 is fixed on the other end of the beam. The torsion pendulum is suspended by a 25-μm tungsten wire about 513 mm long and enclosed in a stainless vacuum vessel maintained at a vacuum of 2×10^{-5} Pa by an ion pump near the suspension point of the wire. The height and direction of the pendulum can be adjusted by a vacuum feedthrough.

The construction of an aluminum bench used to hold the attracting masses is also shown in Fig. 1. The bench was manufactured very carefully with consideration of its symmetries about central lines and the residual strain. Two U-shaped notches, which are perpendicular to each other, but at different levels, were milled on the upper surface of the bench. One of them is used to hold the cylinders in positions, and the other is used to install the gauge blocks. There is a hole in the vertical direction at the symmetrical center of the bench, which is used to fix the bench with the rotary table. The separation of the cylindrical masses M_A and M_B is adjusted and measured against two equal-gauge blocks. The length of each gauge block is 60.240 mm with an uncertainty of 0.001 mm, and so the uncertainty of separation between the opposite face of M_A and M_B was less than 0.002 mm. As a result of the precisely machined U-shaped notch, the axes of the attracting masses are coincident in the range of less than 1×10^{-5} rad. The rotary table can be located at any angle by means of a stepper motor and servocontrol system, and 72000 steps will drive the table to make one revolution. We can use this system to make the coaxial line of the attracting masses perpendicular to the beam of the pendulum. The experiments showed that the coaxial line of the masses was perpendicular to the beam with uncertainty less than $\alpha_0=5\times10^{-3}$ rad, which is at least partly due to imperfection of the rotary table. The rotary table was installed on a massive displacement device, which can be adjusted precisely in two horizontal coordinates. In order to ensure that m_1 is centered between the attracting masses, we can detect the changes of equilibrium point of the pendulum with and without the attracting masses in places, and then adjust the displacement device. The position uncertainties of m_1 in the center between attracting masses in the horizontal directions

TABLE I. Dimensions and masses of attracting cylinders and pendulum.

Parameter	Value
Length of M_A (L_A)	(100.007±0.001) mm
Length of M_B (L_B)	(100.000±0.001) mm
Diameter of M_A	(100.003±0.001) mm
Diameter of M_B	(99.998±0.001) mm
Mass of M_A	(6.2513 3±0.00001) kg
Mass of M_B	(6.2505 6±0.00001) kg
Separation between M_A and M_B ($2d$)	(60.240±0.002) mm
Mass of sphere m_1	(32.2560±0.0005) g
Mass of sphere m_2	(32.2858±0.0005) g
Horizontal distance between m_1 or m_2 and the suspension point (b)	(200.000±0.001) mm
Length of A	(403.998±0.004) mm
Diameter of A	(4.930±0.001) mm
Length of B	(19.991±0.001) mm
Diameter of B	(5.951±0.001) mm
Mass of A and B (together)	(21.9461±0.0005) g
Height of C	(22.802±0.001) mm
Diameter of C	(14.104±0.001) mm
Height of D	(10.997±0.001) mm
Diameter of D	(5.996±0.001) mm
Mass of C and D (together)	(9.6859±0.0005) g

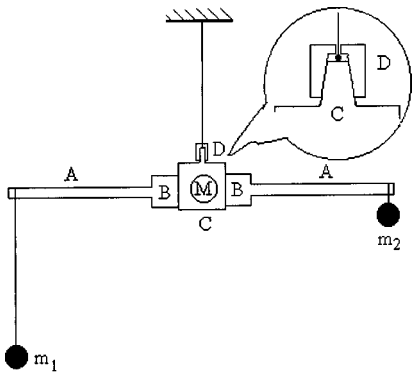

FIG. 2. Detail structure of the torsion pendulum.

were less than 0.01 mm and in the vertical direction were less than 0.5 mm.

The detailed structure of the torsion pendulum is shown in Fig. 2. The aluminum torsion pendulum beam consists of five parts, marked *A*, *B*, *C*, *D*, and *M*, respectively. The diameter of part *A* of the pendulum beam is about 1 mm thinner than that of the center part marked *B* of the beam: so the long beam can go through the cylindrical hole on the cylinder *C* more easily. A very small hole was pierced through the center of top cylinder *D*, and a tungsten fiber of 25 μm in diameter can just pass through it. Then the fiber was tied and twisted a knot with a short length of thin copper wire. Part *D* was taper fit with part *C*, as shown in Fig. 2. The cylinder *C* was cut into two small pieces on both sides for attaching the reflection mirrors *M*. The test masses m_1 and m_2 are hung by the tungsten fibers of 50 μm in diameter through the small V-shaped notches on the two ends of beam. The dimensions of beam are also listed in Table I. The lengths and diameters were measured by the micrometers and an improved Abbe Comparator.

The rotation of the torsion pendulum is detected by an optical lever in which the light beam from a He-Ne laser of 2.5 mW passes through a chopper with a frequency of 731 Hz and is reflected by the mirror *M* and then falls on a position-sensitive photocell (SD-1166-21-11-391, made by Silicon Detector Corporation, Newbury Park), which is placed about 2 m far from the mirror. The difference signal voltage from the position sensor goes through a lock-in amplifier (128A, EG&G Company, Princeton), and then it is plotted by an *X*-*Y* chart recorder (type 3033, made by Sichuan No. 4 Instrument Factory, Chongqing, China) in analog form continuously and is digitized by a 586 microcomputer each second. The square wave signal of 100 kHz output from a high-stability quartz oscillator (EE1610A, made by Nanjing Telecommunication Instruments Factory, Nanjing, China) was divided to 1 Hz by means of a transistor-transistor-logic (TTL) frequency-division circuit. It was considered as a standard clock reference and used to control the computer sampling and save the data output from the analog-to-digital (A/D) converter. The clock reference was checked by a Universal Time Interval Counter (SR620, made by Stanford Research Systems Company, Sunnyvale), and its frequency stability reaches in the order of 2×10^{-9}/day. The amplitude of the rotation of the pendulum was about 2×10^{-3} rad. Long-term observations have shown that the linear drift of the fiber, which has been suspended for 2 yr, was approximately 2×10^{-6} rad/day. The corresponding period drifts of the pendulum were about 74 ms/day and 57 ms/day when the attracting masses were on and off positions, respectively.

The apparatus was located in a mu-metal shielded room of 5 m$\times$3 m$\times$3.5 m in dimension, and all materials used in the experiment such as the pendulum beam, the attracted, and counterweight masses as well as the attracting cylinders were either diamagnetic or paramagnetic, which can greatly reduce the possible effects due to the magnetic fields. In order to test for magnetic effects, a small coil was set close to the vacuum tube near the test mass and the equilibrium point of the torsion pendulum was measured [15]. The result showed that the magnetic effect could be neglected in our experiment. The room is installed on a shock-proof platform that weighs about 24 tons, and the platform is supported by 16 thick springs. The natural frequency of this system is about 2 Hz. Under the ground of our laboratory about 3 m deep, there is a ground net connected with thick copper plates and wires. The laboratory is located in the center of Yu-Jia Mountain, which is in north of our campus (HUST). The least thickness of the cover on the laboratory is more than 40 m, and the exit is at the foot of the mountain and 150 m away from the laboratory. The daily change of temperature in the shielding room of our cave laboratory is less than 0.005 °C [16].

III. NONLINEAR FITTING PERIOD

In our experiment, the periods of pendulum were about 4441 s and 3484 s with and without the attracting masses in positions, respectively, and the period change was about 27%. Another advantage of this configuration is that the relative uncertainty due to the limitation of measuring dimensions of the beam and mirror will be reduced because of the longer beam. But as is well known, this configuration will induce serious nonlinear effects due to the long torsion beam and different height of the attracted masses in the inhomogeneous gravitational fields. To consider the nonlinear effect, the equation of torsion pendulum motion should be written as

$$I\ddot{\theta}+k_1\theta+k_2\theta^2+k_3\theta^3=0, \tag{7}$$

where $k_1=K_f+K_g+K_b$ or $k_1=K_f+K_b$ in the case of attracting masses on or off positions; k_2 and k_3 are usually much smaller than k_1. The approximate solution of Eq. (7) is

$$\theta(t)\approx\theta_0\ \sin\ \omega t-\frac{k_2}{6k_1}\ \theta_0^2(\cos 2\omega t+3)-\frac{k_3}{32k_1}\ \theta_0^3\ \sin 3\omega t, \tag{8}$$

where θ_0 is the oscillation amplitude. The frequency ω is shifted from its unperturbed value $\omega_0^2=k_1/I$ by

$$\omega^2=\omega_0^2[1+3k_3\theta_0^2/(4k_1)]. \tag{9}$$

Data were taken alternately with and without the attracting cylindrical masses in position, and each set of runs which

TABLE II. $\Delta(\omega_0^2)$ determined by the nonlinear fitting method for different sets.

Set No.	Duration of run (hour/day/month)	$\Delta(\omega_0^2)$ ($\times 10^{-6}$ s^{-2})
	On: 09:00/04/Aug.–08:15/06/Aug.	
1	Off: 09:20/07/Aug.–09:25/09/Aug.	−1.250654
	On: 10:12/25/Aug.–15:40/27/Aug.	
2	Off: 16:10/28/Aug.–16:50/30/Aug.	−1.250632
	On: 07:00/31/Aug.–08:30/02/Sept.	
3	Off: 23:40/02/Sept.–23:15/04/Sept.	−1.250625
	On: 11:10/13/Sept.–10:30/15/Sept.	
4	Off: 11:30/16/Sept.–12:00/18/Sept.	−1.250508
	On: 10:30/23/Sept.–07:10/25/Sept.	
5	Off: 23:00/25/Sept.–12:30/27/Sept.	−1.250585
	On: 13:40/01/Oct.–15:20/03/Oct.	
6	Off: 14:05/04/Oct.–18:45/06/Oct.	−1.250688
	On: 16:00/08/Oct.–05:30/11/Oct.	
7	Off: 15:35/12/Oct.–06:25/15/Oct.	−1.250813
	Average	−1.250644
	Uncertainty	0.000094

lasted about a week was correspondingly separated into two groups. The frequencies for each of the individual groups (2 or 3 days) were extracted from the angle-time data of the pendulum by the nonlinear least-squares fitting method. We used the following function:

$$\theta(t)=a_1\sin(\omega t+\varphi_1)+a_2\sin(2\omega t+\varphi_2)+a_3\sin(3\omega t+\varphi_3)+bt+b_0 \quad (10)$$

to fit the raw data. A similar nonlinear fitting method has been used in testing the equivalence principle by Gundlach *et al.* [17]. The results of fitting data showed that φ_3 was about 3 times φ_1, which is consistent with the theoretical result. This means that if we select the initial time as φ_1/ω, Eq. (10) can be simplified as Eq. (8). From Eqs. (8), (9), and (10), we can obtain

$$\omega_0^2=\omega^2/(1-24a_3/a_1). \quad (11)$$

The results of fitting data also showed that a_3/a_1 were about 1.08×10^{-5} and 1.81×10^{-5} when attracting masses were off and on positions; so ω_0^2/ω^2 was about 1.000259 and 1.000434 in those two cases, and the upward fractional bias in G due to this was about 21.0 ppm. This bias was mainly contributed by the nonlinearity in the torque contribution of the attracting masses, which is about 13 ppm in theoretical calculation and may be partly contributed by the other systematic error sources, such as the nonlinearities of the position sensor and the background gravitational field. Table II lists the $\Delta(\omega_0^2)$ determined by the nonlinear fitting method.

The nonlinearity of the position sensor was measured through changing its position stably and slowly by means of the Abbe Comparator while the light beam of the laser was fixed. Figure 3 showed the output transfer characteristic of the position sensor. We also used the function

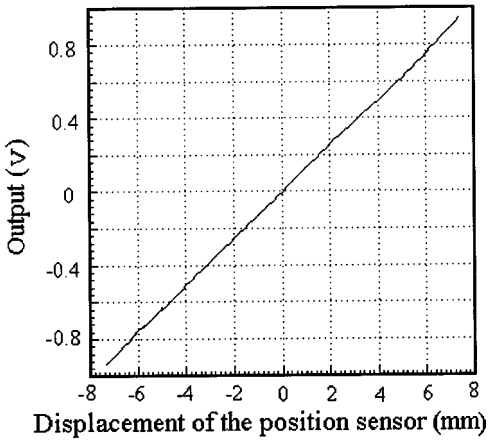

FIG. 3. Output transfer characteristic of the position sensor.

$$V(x)=b_1x+b_2x^2+b_3x^3+b_0, \quad (12)$$

to fit the data of the output transfer characteristic of the position sensor, and obtained $b_2/b_1=5.41\times10^{-5}$ mm^{-1}, $b_3/b_1=3.99\times10^{-4}$ mm^{-2}. However, these results only set an upper limit on the nonlinearity of the position sensor because the accuracy of the Abbe Comparator is about 1 μm and the relative uncertainty in a displacement measurement of a few millimeters is on the order of 10^{-4}. If these results were considered as the nonlinearity of the detector, the ratio a_3/a_1 should be about 0.006. But as we have indicated, the results of fitting data showed that a_3/a_1 was about 1.08×10^{-5} and 1.81×10^{-5} when attracting masses were off and on positions. This strongly implies that the detector is much more linear than the upper limitation given above.

Because the quality factor of torsion pendulum Q in our case is approximately 3.6×10^4, it is believed that both frequency changes resulting from the damping and systematic bias due to the fiber anelasticity predicted by Kuroda can be neglected [12].

IV. EXPERIMENTAL RESULTS

In the Cartesian coordinate system (x,y,z) as shown in Fig. 4, the center of the right and left faces of two cylinders can be expressed as

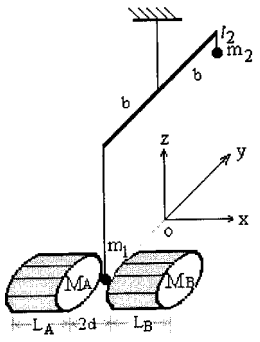

FIG. 4. Coordinate system of the pendulum.

$$\begin{cases} x_{AL}=x_0-d-L_A, \\ x_{AR}=x_0-d, \\ y_{AL,R}=y_0-b, \\ z_A=z_0, \end{cases} \quad \begin{cases} x_{BL}=x_0+d, \\ x_{BR}=x_0+d+L_B, \\ y_{BL,R}=y_0-b, \\ z_B=z_0, \end{cases} \tag{13}$$

where (x_0,y_0,z_0) are uncertainties of the position of m_1 in the center between the attracting masses in the three axes. The gravitational torsion constant of a point mass which at point (x,y,z) can be expressed in two parts:

$$\begin{aligned} C_{gt}=&2m\rho_A[C_t(x-x_{AL},R_A,s_A)-C_t(x-x_{AR},R_A,s_A)]x+2m\rho_B[C_t(x_{BL}-x,R_B,s_B)-C_t(x_{BR}-x,R_B,s_B)]x \\ &+2m\rho_A\left[\frac{\partial C_t(x-x_{AR},R_A,s_A)}{\partial(x-x_{AR})}-\frac{\partial C_t(x-x_{AL},R_A,s_A)}{\partial(x-x_{AL})}\right]y^2-2m\rho_B\left[\frac{\partial C_t(x_{BR}-x,R_B,s_B)}{\partial(x_{BR}-x)}-\frac{\partial C_t(x_{BL}-x,R_B,s_B)}{\partial(x_{BL}-x)}\right]y^2 \\ &-2m\rho_A\left[\frac{\partial C_t(x-x_{AR},R_A,s_A)}{\partial s_A}-\frac{\partial C_t(x-x_{AL},R_A,s_A)}{\partial s_A}\right]xyy_A\Big/ s_A \\ &+2m\rho_B\left[\frac{\partial C_t(x_{BR}-x,R_B,s_B)}{\partial s_B}-\frac{\partial C_t(x_{BL}-x,R_B,s_B)}{\partial s_B}\right]xyy_B\Big/ s_B, \end{aligned} \tag{14}$$

$$\begin{aligned} C_{gr}=&+2m\rho_A[C_r(x-x_{AL},R_A,s_A)-C_r(x-x_{AR},R_A,s_A)](x^2h_A^2-yy_As_A^2)/s_A^3 \\ &-2m\rho_B[C_r(x_{BL}-x,R_B,s_B)-C_r(x_{BR}-x,R_B,s_B)](x^2h_B^2+yy_Bs_B^2)/s_B^3 \\ &+2m\rho_A\left[\frac{\partial C_r(x-x_{AR},R_A,s_A)}{\partial(x-x_{AR})}-\frac{\partial C_r(x-x_{AL},R_A,s_A)}{\partial(x-x_{AL})}\right]xyy_A\Big/ s_A \\ &+2m\rho_B\left[\frac{\partial C_r(x_{BR}-x,R_B,s_B)}{\partial(x_{BR}-x)}-\frac{\partial C_r(x_{BL}-x,R_B,s_B)}{\partial(x_{BL}-x)}\right]xyy_B\Big/ s_B \\ &-2m\rho_A\left[\frac{\partial C_r(x-x_{AR},R_A,s_A)}{\partial s_A}-\frac{\partial C_r(x-x_{AL},R_A,s_A)}{\partial s_A}\right]x^2y_A^2\Big/ s_A^2 \\ &-2m\rho_B\left[\frac{\partial C_r(x_{BR}-x,R_B,s_B)}{\partial s_B}-\frac{\partial C_r(x_{BL}-x,R_B,s_B)}{\partial s_B}\right]x^2y_B^2\Big/ s_B^2, \end{aligned} \tag{15}$$

where ρ_A and ρ_B are the densities of the attracting cylinders, and

$$\begin{cases} y_A=y-y_{AL,R}, \\ y_B=y_{BL,R}-y, \end{cases} \quad \begin{cases} h_A=z-z_A, \\ h_B=z-z_B, \end{cases} \quad \begin{cases} s_A=\sqrt{y_A^2+h_A^2}, \\ s_B=\sqrt{y_B^2+h_B^2}. \end{cases} \tag{16}$$

The $C_t(x,R,s)$ and $C_r(x,R,s)$ are the function of axial and radial gravitational attracting of a finite cylinder, which are given in Refs. [18] and [19], and can be expressed as follows:

$$\begin{aligned} C_t(x,R,s)=&-s\pi+\frac{R^2-x^2-s^2}{\sqrt{(R+s)^2+x^2}}K(k)+\sqrt{(R+s)^2+x^2}E(k) \\ &+\frac{x^2}{\sqrt{(R+s)^2+x^2}}\left[\frac{\sqrt{x^2+s^2}+R}{\sqrt{x^2+s^2}-s}\prod(p_1,k)+\frac{\sqrt{x^2+s^2}-R}{\sqrt{x^2+s^2}+s}\prod(p_2,k)\right], \end{aligned} \tag{17}$$

$$C_r(x,R,s)=\frac{x^2}{2s\sqrt{1+(R+s)^2/x^2}}\left\{\left[1+2\frac{R^2+s^2}{x^2}\right]K(k)-\left[1+\frac{(R+s)^2}{x^2}\right]E(k)-\frac{(R-s)^2}{x^2}\prod(h,k)\right\}, \tag{18}$$

where

$$k=\sqrt{\frac{4sR}{(R+s)^2+x^2}}, \quad p_1=\frac{2s}{\sqrt{x^2+s^2}-s}, \quad p_2=\frac{-2s}{\sqrt{x^2+s^2}+s}, \quad h=-\frac{4sR}{(R+s)^2},$$

TABLE III. Error budget.

Source of uncertainty		Uncertainty of G in ppm
Position of the attracting masses		
	$\Delta d = 0.002$ mm	48
	$\chi_0 = 0.01$ mm	4.2
	$y_0 = 0.01$ mm	25
	$z_0 = 0.5$ mm	16
	$\alpha_0 = 5 \times 10^{-3}$ rad	24
Density of the attracting masses		17
Mass of the attracted masses		16
Moment of inertia of pendulum		31
Nonlinearity of the systematic error sources		8
$\Delta(\omega_0^2)$		75
Total		105

and $K(k)$, $E(k)$, and $\Pi(p_1,k)$ [or $\Pi(p_2,k)$] here are the complete elliptical integrals of the first, second, and third kinds respectively.

The gravitational torsion constant C_g can be calculated by integrating C_{gt} and C_{gr} over all parts of the pendulum. When selecting $x_0=0$, $y_0=0$, $z_0=0$, and $\theta=0$, we calculated contributions to C_g from the attracted mass, counterweight mass, and pendulum beam with mirrors as -53.8673 kg^2 m^{-1}, -0.0860 kg^2 m^{-1}, and 0.0136 kg^2 m^{-1}, respectively. So the total gravitational torsion constant C_g was -53.9397 kg^2 m^{-1}. For the same reason, we obtained that the relative uncertainty of C_g due to the position of attracting masses was 62 ppm, which is listed in the first five rows of Table III, and the relative uncertainties of densities of attracting cylinders and mass of attracted balls based on the parameters in Table I were 17 ppm and 16 ppm, respectively. These uncertainties were contributed to the relative uncertainty of G directly as listed in sixth and seventh rows of Table III.

The density of the aluminum beam is $\rho_{\mathrm{Al}}=(2.7828 \pm 0.0001)$ g/cm^3, and we obtained the moments of the pendulum beam with mirrors and the attracted masses as follows:

$$I_{\mathrm{beam}}=(0.29203\pm 0.00003)\times 10^{-3}\ \mathrm{kg\ m^2}, \tag{19}$$

$$I_m=(2.58466\pm 0.00006)\times 10^{-3}\ \mathrm{kg\ m^2}. \tag{20}$$

So the total moment of the pendulum is $I=2.87669 \times 10^{-3}$ kg m^2 with relative uncertainty of 31 ppm, which is listed in the eight row of Table III. The value for G determined finally is $(6.6699\pm 0.0007)\times 10^{-11}$ m^3 kg^{-1} s^{-2}.

The experimental result showed that the nonlinear effects could be effectively subtracted from the angle-time data of the pendulum by a suitable nonlinear least-squares fitting method, although our torsion pendulum system was designed to be sensitive to the inhomogenous gravitational fields. Of course, further improvement of G is mainly limited by the uncertainty of measuring the frequencies of the torsion pendulum, as shown in Table III, in our experiment. We are going to design a new torsion pendulum system and employ the optimum positioning of the the pendulum and attracting masses to reduce the nonlinear effects in the experiment [11], and hope to get a value of G with higher precision.

ACKNOWLEDGMENTS

We would like to thank Y. Z. Zhang of the Institute of Theory Physics of Academic Sinica and H. T. Hsu of the Institute of Geodesy and Geophysics of Academic Sinica for their valuable discussions. We are also grateful to the National Natural Science Foundation of China for Financial Support, under Grants 19425008 and 19375019.

[1] G. T. Gillies, Rep. Prog. Phys. **60**, 151 (1997).
[2] A. Cornaz, B. Hubler, and W. Kündig, Phys. Rev. Lett. **72**, 1152 (1994).
[3] H. Walesch, H. Meyer, H. Piel, and J. Schurr, IEEE Trans Instrum. Meas. **44**, 491 (1995).
[4] M. P. Fizgerald and T. R. Armstrong, IEEE Trans Instrum. Meas. **44**, 494 (1995).
[5] W. Michaelis, H. Haars, and R. Augustin, Metrologia **32**, 267 (1995/96).
[6] P. R. Heyl, J. Res. Natl. Bur. Stand. **5**, 1243 (1930); P. R. Heyl and P. Chrzanowski, *ibid.* **29**, 1 (1942).
[7] G. G. Luther and W. R. Towler, Phys. Rev. Lett. **48**, 121 (1982).
[8] J. H. Gundlach, E. G. Adelberger, B. R. Heckel, and H. E. Swanson, Phys. Rev. D **54**, R1256 (1996).
[9] K. Kuroda and M. A. Borton, Int. J. Mod. Phys. A **12**, 1967 (1997).
[10] Y. T. Chen, Phys. Lett. **106A**, 19 (1984).
[11] Z. K. Hu and J. Luo, Phys. Lett. A **238**, 337 (1998).
[12] K. Kuroda, Phys. Rev. Lett. **75**, 2796 (1995).
[13] C. H. Bagley and G. G. Luther, Phys. Rev. Lett. **78**, 3047 (1997).
[14] Y. T. Chen, A. H. Cook, and A. J. F. Metherell, Proc. R. Soc. London **A394**, 47 (1984).
[15] S. H. Fan, J. Tang, and J. Luo, College Phys. (in Chinese) **15**, 27 (1996).
[16] S. H. Fan, S. C. Wu, and J. Luo, Rev. Sci. Instrum. **68**, 3079 (1997).
[17] J. H. Gundlach, G. L. Smith, E. G. Adelberger, B. R. Heckel, and H. E. Swanson, Phys. Rev. Lett. **78**, 2523 (1997).
[18] Y. T. Chen and A. H. Cook, Phys. Lett. A **138**, 378 (1989).
[19] J. Luo, X. R. Zhang, J. G. Li, S. H. Fan, and P. H. Zhang, Sci. China, Ser. A **33**, 1214 (1990).